ACS EARTH AND SPACE CHEMISTRY

http://pubs.acs.org/journal/aesccq

Article

Biological Influence on $\delta^{13}C$ and Organic Composition of Nascent Sea Spray Aerosol

Daniel R. Crocker, Ritchie E. Hernandez, Haonan D. Huang, Matthew A. Pendergraft, Ruochen Cao, Jiayin Dai, Clare K. Morris, Grant B. Deane, Kimberly A. Prather,* and Mark H. Thiemens*

Cite This: *ACS Earth Space Chem.* 2020, 4, 1686–1699

Read Online

ACCESS | Metrics & More | Article Recommendations | Supporting Information

ABSTRACT: Elucidating the influence of oceanic biological activity on the organic composition of sea spray aerosol (SSA) is crucial to understanding marine cloud properties relevant to climate. Numerous marine field studies designed to address this topic have yielded conflicting results mainly as a result of the inability to distinguish primary SSA composition from terrestrial and marine secondary organic aerosols. In this study, two laboratory-induced phytoplankton blooms were conducted in an isolated system without background aerosol contributions. Values for $\delta^{13}C$ were measured for SSA ($\delta^{13}C_{SSA}$) along with seawater particulate and dissolved organic carbon ($\delta^{13}C_{POC}$ and $\delta^{13}C_{DOC}$) to track changes in carbon transfer and composition between seawater and SSA. Contrary to common assumptions, $\delta^{13}C_{SSA}$ values were not equivalent to $\delta^{13}C_{DOC}$. The consistently less negative $\delta^{13}C_{SSA}$ values indicate that nascent $\delta^{13}C_{SSA}$ reflects specific changes in relative contributions to SSA from the available seawater carbon pools, as a function of biological activity. A dual-source isotopic mixing model revealed that the difference between $\delta^{13}C_{SSA}$ and $\delta^{13}C_{DOC}$ was explained by increased relative contributions of "freshly produced" organic carbon (OC) to SSA, with the largest contribution of "freshly produced" OC occurring 2−3 days after the maximum chlorophyll-*a* concentrations. This finding is consistent with previous mesocosm studies, showing that organic enrichment in SSA requires processing by heterotrophic bacteria after periods of high primary productivity. This work examining the biological influences on SSA organic composition and nascent $\delta^{13}C_{SSA}$ values provides new insights into ocean-to-SSA carbon transfer dynamics, which can be used in future field studies to improve estimates of anthropogenic influences on the carbon composition of the marine environment.

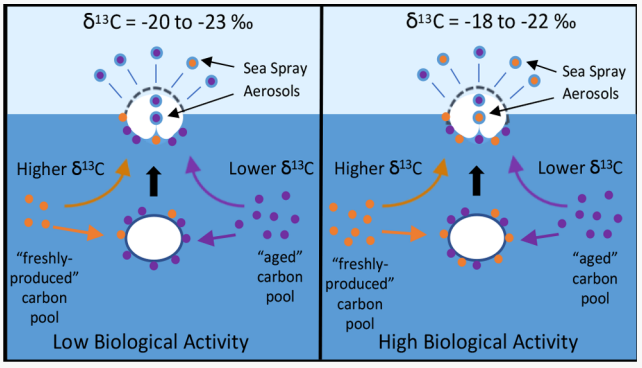

KEYWORDS: *carbon isotopes, sea spray aerosol, particulate organic carbon, dissolved organic carbon, phytoplankton bloom, sea surface microlayer, aerosol source apportionment*

INTRODUCTION

Sea spray aerosol (SSA), formed by bubbles bursting at the ocean surface, is one of the most abundant aerosol types globally.[1,2] SSA covers a broad size range from 0.01 to >10 μm in diameter[3] and consists of complex mixtures of inorganic ions, organic molecules, and marine microorganisms (e.g., phytoplankton, bacteria, and viruses) found in the ocean.[4−6] Earth's radiative budget is impacted by SSA through direct scattering of sunlight and seeding clouds,[7−9] and the extent to which SSA affects the Earth's radiative budget depends upon the particle size, number concentration, and chemical composition. Higher SSA organic carbon (OC_{SSA}) content has been shown to decrease hygroscopic growth factors and reduce the light-scattering ability of SSA.[10] Additionally, the ice nucleation ability of SSA is strongly controlled by specific organic and biological species,[11] highlighting the importance of chemical composition to predict the impact of SSA on clouds and climate.

The basic principles controlling SSA formation and organic enrichment have been extensively studied with air entrainment from breaking waves forming bubbles, which then rise, scavenging organic material during their ascent to the air−sea interface.[12−14] SSA is formed primarily by two separate mechanisms when bubbles burst at the ocean surface. Film drops, which are mostly sub-micrometer in size, are formed from the bursting of the bubble film, the top part that protrudes from the ocean surface.[15] Jet drops are formed from the collapse of the bubble cavity and represent the majority of

Special Issue: Marine Particle Chemistry: Influence on Biogeochemical Cycles and Particle Export

Received: March 14, 2020
Revised: July 28, 2020
Accepted: August 7, 2020
Published: August 7, 2020

https://dx.doi.org/10.1021/acsearthspacechem.0c00072
ACS Earth Space Chem. 2020, 4, 1686−1699

super-micrometer SSA as well as contributing some to sub-micrometer SSA.[15] Because SSA formation takes place at the air−sea interface, the sea surface microlayer (SSML), the top 1−1000 μm of the ocean enriched with organic compounds, plays an integral role in ocean-to-SSA transfer of organic species.[16,17] The SSML forms on the ocean surface at low wind speeds in tropical and subtropical regions.[18] Organic material accumulates on the bubble surface during its ascent, and organic species in the SSML are concentrated on the bubble film, leading to an enrichment of organic matter in SSA, especially sub-micrometer film drops, once the bubbles burst at the air−sea interface.

Despite the abundance of research addressing transfer processes of organic species into SSA, the relationship between oceanic biological activity (i.e., phytoplankton blooms) and SSA chemical composition remains a highly debated topic among researchers.[13,19−24] As the main primary producers in the ocean, phytoplankton convert inorganic CO_2 to organic biomass. Initially, most of this "freshly produced" organic biomass is particulate organic carbon (POC), operationally defined as organic particles of >0.7 μm in diameter.[25] During initial bloom growth, POC consists mostly of whole, living phytoplankton, and the emergence of large bacteria and organic aggregates also contributes to POC biomass after the initial growth phase.[25−27] As a bloom progresses, phytoplankton exudates, death, and bacterial processing result in degradation of "freshly produced" organic material to smaller sizes of <0.7 μm, termed the dissolved organic carbon (DOC) pool.[19,27] Degradation of this organic material continues long after phytoplankton bloom senescence, resulting in an abundance of older, "aged" OC, most of which is DOC, in oceanic regimes with low biological activity.

Because "aged" OC is far more abundant than "freshly produced" OC in most oceanic regimes, some researchers have concluded "aged" OC is the only important carbon pool that contributes to OC_{SSA}.[13,19,20] Contrary to this, many field measurements indicate that OC_{SSA} concentrations correlate with primary productivity and track with chlorophyll *a* (chl *a*), implying a substantial contribution of "freshly produced" OC to SSA in oceanic regimes of high biological activity.[21−24] To resolve these discrepancies between field studies, it would be prudent to elucidate the contribution of "freshly produced" OC to OC_{SSA}. However, in the marine environment, this is complicated by numerous factors, including formation of marine secondary organic aerosol (SOA), interference from terrestrial aerosol sources, chemical transformations during atmospheric transport, and bacterial enzymatic degradation of labile, "freshly produced" OC in the seawater.[28−32] The first two factors contribute interfering marine aerosol carbon with an organic composition different from pure SSA, while the latter two can obscure chemical distinctions between newer, "freshly produced" and older, "aged" OC in SSA. A recent mesocosm study focusing on the effects of seawater biology on SSA chemical composition found that enrichment of aliphatic organics in SSA was different for two consecutive phytoplankton blooms and controlled by the bacterial enzymatic activity in the seawater as well as microbial degradation of "freshly produced" OC.[32] The variability in conclusions drawn from the abundance of research highlights the necessity for laboratory studies of isolated, nascent SSA to provide insight into ocean-to-SSA organic transfer during periods of high biological activity and identify the seawater carbon sources contributing to OC_{SSA}.

Stable carbon isotopic analysis is an excellent technique for identifying and quantifying sources of carbon species. To date, the primary application of stable carbon isotopic measurements ($\delta^{13}C$) to marine aerosols has been for source apportionment to determine the fractional contributions of OC_{SSA} (f_{SSA}) versus anthropogenic aerosol carbon (f_{anth}) to the marine environment. These source apportionment calculations are made using a dual-source isotopic mixing model (eq 1) with the assumption that the two sources contributing to aerosol carbon in the marine environment are SSA and anthropogenic aerosols.[33−39]

$$\delta^{13}C_{marine} = (f_{SSA})(\delta^{13}C_{SSA}) + (f_{anth})(\delta^{13}C_{anth}) \quad (1)$$

The calculation requires precise knowledge of the nascent SSA carbon isotopic composition ($\delta^{13}C_{SSA}$), but determination of this value in the marine environment is complicated by photochemical aging of primary SSA, formation of marine SOA, and contributions from terrestrial aerosols. Historically, because "aged" OC is the most abundant surface ocean OC reservoir, most studies assume that $\delta^{13}C_{SSA}$ is the same as $\delta^{13}C$ for seawater DOC, from around −20 to −23‰.[37−39] This assumption has come under scrutiny recently, with measurements of primary marine aerosols in the North Atlantic indicating a trend of less negative $\delta^{13}C$ values during periods of high biological activity.[34] The researchers attributed this to incorporation of "freshly produced" organic species into SSA. Additional isotopic studies on marine aerosols led to the proposal that two distinct carbon pools, nominally "freshly produced" and "aged" OC, were both contributing to OC_{SSA}.[40] The study, however, did not include seawater $\delta^{13}C_{POC}$ and $\delta^{13}C_{DOC}$ measurements that may have allowed for quantification of their relative contributions.

Building upon previous research, this study aims to quantify the contribution of "freshly produced" OC to OC_{SSA} by combining $\delta^{13}C_{SSA}$ measurements with seawater $\delta^{13}C_{POC}$ and $\delta^{13}C_{DOC}$ measurements. Often during phytoplankton blooms, significant $\delta^{13}C$ increases of 3−5‰ occur in "freshly produced" OC, leading to $\delta^{13}C$ for "freshly produced" OC that is isotopically distinct from $\delta^{13}C$ values for "aged" OC.[41,42] This is due to either less ^{12}C isotopic discrimination by phytoplankton during CO_2 fixation or phytoplankton fixation of isotopically heavier (less negative) bicarbonate as competition increases for available CO_2.[41−43] It was stated above that generally in the marine environment "freshly produced" OC is predominantly POC, while the majority of "aged" OC is DOC. When this is the case, the $\delta^{13}C$ values for "freshly produced" and "aged" OC can be approximated with measurements of seawater $\delta^{13}C_{POC}$ and $\delta^{13}C_{DOC}$. Therefore, eq 2a, a dual-source isotopic mixing model analogous to eq 1, allows for calculation of the fractional contribution for "freshly produced" OC to OC_{SSA} (eq 2b).

$$\delta^{13}C_{SSA} = (f_{fresh\ OC})(\delta^{13}C_{POC}) + (f_{aged\ OC})(\delta^{13}C_{DOC}) \quad (2a)$$

$$\frac{\delta^{13}C_{SSA} - \delta^{13}C_{DOC}}{\delta^{13}C_{POC} - \delta^{13}C_{DOC}} = \text{fraction}_{fresh\ OC} \quad (2b)$$

In this study, two separate phytoplankton blooms were induced by nutrient addition to an isolated system containing natural seawater. Carbon concentrations and $\delta^{13}C$ values for POC, DOC, SSML, and SSA were measured along with phytoplankton and bacterial abundance to elucidate the

https://dx.doi.org/10.1021/acsearthspacechem.0c00072
ACS Earth Space Chem. 2020, 4, 1686−1699

contributions to SSA from "freshly produced" and "aged" organic material. For these experiments, "freshly produced" OC refers to organic material produced during the phytoplankton bloom experiments and "aged" OC refers to organic material present in the initial seawater before nutrient addition. The findings confirm previous research indicating a significant contribution of "freshly produced" OC to OC_{SSA}, providing insight into how biological activity impacts nascent $\delta^{13}C_{SSA}$ values in the marine environment and ocean-to-SSA carbon dynamics.

EXPERIMENTAL METHODS

Marine Aerosol Reference Tank (MART) Bloom Experiments. Two separate phytoplankton bloom experiments, henceforth referred to as MART1 and MART2, were carried out in the same MART system for 2−3 weeks each.[44] In each experiment, the 210 L tank was filled with 120 L of natural, filtered (50 μm Nitex mesh to remove zooplankton) seawater collected from Ellen Browning Scripps Memorial Pier (32.8634° N, 117.2546° W) on April 23, 2018 and May 31, 2018 for MART1 and MART2, respectively. After seawater was added, a water chiller was attached to maintain a constant water temperature of 18 °C throughout the experiment, the first chl *a* measurement was made, and the seawater was left overnight to equilibrate. The next morning, initial samples of DOC, POC, and SSML were collected, followed by the addition of Guillard's f/20 diatom growth medium with sodium metasilicate[45] and the activation of solar simulator lamps to continuously supply ∼70 μE m^{-2} s^{-1} photosynthetically active radiation to the MART for biological growth.[46] Phytoplankton speciation was not determined for these experiments, and microbial communities in the initial seawater were not altered in any way before the addition of growth medium. Keeping the initial seawater unaltered, other than the adding growth nutrients, allows the MART experiments to reproduce the chemical complexity of the open ocean.

To aerate the seawater, particle-free room air was pumped into the MART through Tygon tubing until chl *a*, measured once daily via a calibrated, hand-held fluorometer (Aquafluor, Turner Designs), reached ∼12 μg L^{-1}. The 12 μg L^{-1} threshold has been employed in previous MART experiments to ensure a significant amount of phytoplankton growth before turning on the pump used for water recirculation in the MART, which can lyse fragile cells inhibiting phytoplankton growth.[46] The morning after chl *a* reached ∼12 μg L^{-1}, the Tygon tubing was moved from the seawater to the MART headspace to flow in particle-free air at 6 L min^{-1}. Once particle concentrations in the MART fell below 1 cm^{-3}, aerosol production via the plunging waterfall technique[44] was commenced with a 4 second interval on−off waterfall cycle. The plunging waterfall generates SSA with particle size distributions representative of oceanic wave breaking,[3,44] and a centrifugal pump attached to the MART recirculates water from the bottom of the tank to replenish the waterfall. Extensive methodology and specific chemical and biological details for this type of experiment are described elsewhere.[46]

Sample Collection for SSA, POC, DOC, SSML, and Bacteria. SSA were collected by pulling air from the MART headspace onto 47 mm pre-combusted (500 °C, >4 h) quartz fiber filters at 5 L min^{-1}. A diffusion dryer filled with silica gel was placed before the filters to dry the aerosols before collection. SSA samples consisted of total suspended particles (TSP) collected for >40 h to ensure adequate sample loadings for isotopic measurements. Field blanks were collected at the end of the experiments in addition to 3 day collection filters without aerosol generation (see Methods S1 of the Supporting Information for more details). All SSA samples and blanks were stored at −12 °C in plastic Petri dishes wrapped with Teflon tape. The DOC, POC, SSML organic carbon (OC_{SSML}), and bacteria were collected at the beginning and end of each SSA sampling period. The glass plate method[17] was employed to collect SSML, with care taken to ensure that a 30 cm length of the glass plate was lowered and raised through the seawater at a consistent rate of 5−6 cm/s for every collection.[18] This process was repeated to collect 40 mL of combined seawater and organics in the SSML into a combusted glass vial, corresponding to a SSML thickness of 100 μm across the entire tank surface. The SSML samples were not filtered; therefore, OC_{SSML} contains a combination of both POC and DOC. Bulk seawater was collected from a spigot on the MART located 23 cm below the water surface. The bulk seawater was filtered through a combusted 0.7 μm Whatman glass fiber filter (GF/F) to separate POC from DOC, and two 40 mL DOC aliquots were collected into combusted glass vials. The POC filters were collected into plastic Petri dishes and stored at −12 °C, while SSML and DOC vials were immediately acidified to pH 2, wrapped with Teflon tape, and stored at room temperature. Heterotrophic bacteria in the bulk seawater were enumerated using a BioRad ZE5 flow cytometer after staining with SYBR Green I (catalog S7563, Thermo Fisher).

$\delta^{13}C$ Analysis for SSA, POC, DOC, and SSML. Isotopic analyses are reported in conventional delta notation standardized to Pee Dee Belemnite by eq 3.[47]

$$\delta^{13}C = \left(\frac{\left(\frac{^{13}C}{^{12}C}\right)_{sample}}{\left(\frac{^{13}C}{^{12}C}\right)_{standard}} - 1 \right) \times 1000 \quad (3)$$

SSA Isotopic Analysis. Right after collection, SSA samples and field blanks were cut in half; half was immediately analyzed for $\delta^{13}C$ analysis, and the other half was stored frozen. Following established methods in the Thiemens Stable Isotope Lab at University of California, San Diego (UCSD), the filter half for $\delta^{13}C$ analysis was placed in a 20 cm long quartz tube containing 250 mg of CuO and attached to a vacuum line. After evacuation, a valve was closed to seal the tube, and an 850 °C combustion furnace was placed on the quartz tube for 3 h to convert all carbon to CO_2. CO_2 was then cryogenically separated, the total carbon yield (μmoles of CO_2) was measured by capacitance manometry, and later converted to the OC_{SSA} concentration using the total volume of air collected. Subsequently, CO_2 was collected into a sample tube, and $\delta^{13}C$ analysis was conducted on a MAT 253 isotope-ratio mass spectrometer. SSA samples were not corrected for carbonates; therefore, OC_{SSA} refers to organic carbon and carbonates combined. However, research shows that carbonates have a minimal effect on $\delta^{13}C$ of marine aerosols.[26] Measured SSA concentrations and $\delta^{13}C$ were corrected for filter blanks, as described in Methods S1 of the Supporting Information.

Isotopic Analysis for POC, DOC, and SSML. The OC concentrations and $\delta^{13}C$ values for POC samples were measured at the Scripps Institution of Oceanography Stable Isotope Laboratory using a Thermo Finnigan DeltaPlus

https://dx.doi.org/10.1021/acsearthspacechem.0c00072
ACS Earth Space Chem. 2020, 4, 1686−1699

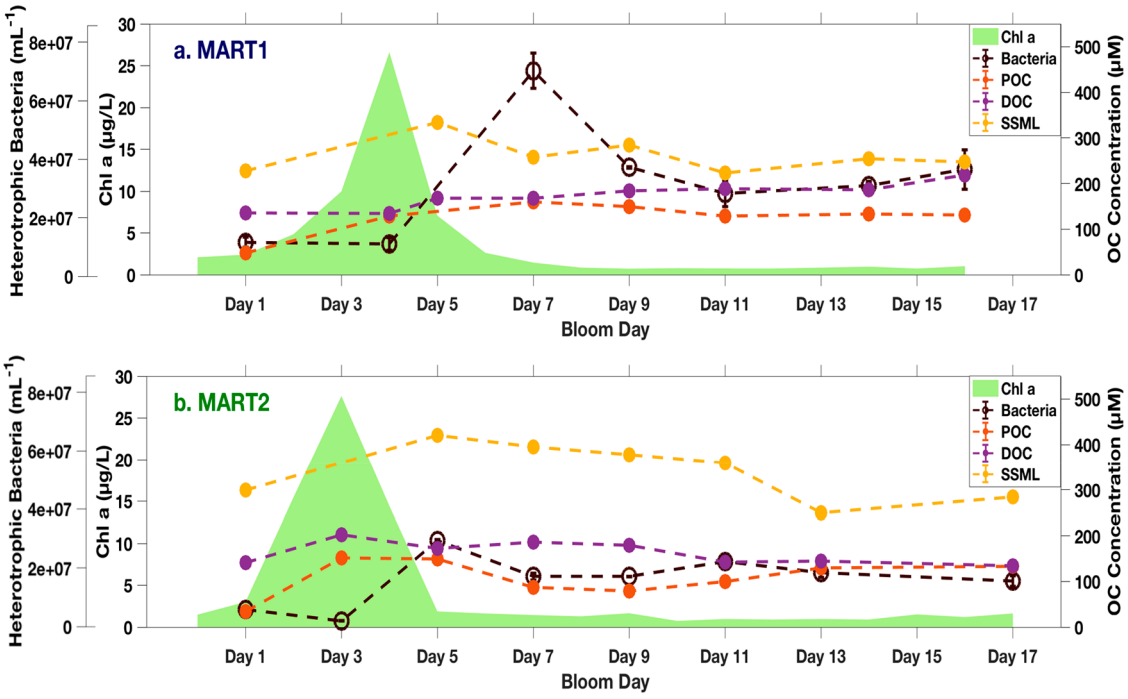

Figure 1. Time series displaying the chl *a*, heterotrophic bacteria, POC, DOC, and OC_{SSML} concentrations for (a) MART1 and (b) MART2. The dashed lines denote that measurements were made at individual time points. The initial DOC measurements for (a) MART1 and (b) MART2 (Day 1) were made before nutrient addition, which contributes 12 μM DOC. Vertical error bars are included for all species, but uncertainty was smaller than the data points for POC, DOC, and OC_{SSML} concentrations.

isotope-ratio mass spectrometer interfaced with a Costech 4010 elemental combustion analyzer. Error analyses were made by measuring GF/F blanks to correct for amounts and isotopes (see Methods S1 of the Supporting Information). SSA isotopic analysis was not carried out on this instrument because OC amounts were below the limit of quantitation. Acidified, liquid DOC and SSML samples were sent to G.G. Hatch Stable Isotope Laboratory in Ottawa, Canada, for $\delta^{13}C$ analysis on an OI Analytical Aurora model 1030 W total organic carbon (TOC) analyzer interfaced to a Finnigan DeltaPlus XP isotope-ratio mass spectrometer with a 1σ analytical precision of ±0.2‰.[48]

Aerosol Size and Mass Measurements. Aerosol size and mass distributions were measured during MART2 (Figure S1 of the Supporting Information) by combining data from a Scanning Mobility Particle Sizer (SMPS, TSI, Inc. model 3936) and an Aerodynamic Particle Sizer (APS, TSI, Inc. model 3321). These measurements demonstrate the consistent aerosol size distributions produced by the MART system and allow for calculation of the total SSA mass concentration. More information on aerosol size measurements and analysis is provided in Methods S2 of the Supporting Information.

Lipid Biomarker Analysis for SSA. Lipid analysis of SSA samples was performed at the UCSD Lipidomics Core. Both lipid-attached and non-esterified (i.e., "free") fatty acids (FAs) were isolated from SSA samples via a conventional Bligh–Dyer extraction.[49] Subsequently, the isolate was saponified to convert lipid-attached FAs to "free" FAs, and all "free" FAs were extracted and derivatized for quantitative analysis on an Agilent 5975 gas chromatography–mass spectrometer. More details for lipid extraction and preparation are given in Methods S3 of the Supporting Information, and a comprehensive description of sample preparation and analysis is available from ref 50.

RESULTS AND DISCUSSION

POC–DOC–OC_{SSA} Dynamics during Phytoplankton Blooms. Phytoplankton bloom progression for both experiments was monitored by measuring the chl *a*, heterotrophic bacteria, POC, DOC, and OC_{SSML} concentrations. These results are shown in Figure 1 and Table S1 of the Supporting Information. Initially, chl *a* was 2.1 μg L^{-1} in MART1 and 1.5 μg L^{-1} in MART2, increasing after nutrient addition to similar maxima of 27 and 28 μg L^{-1}, respectively. These blooms are more intense than most in open marine waters, which typically have peak chl *a* values between 1 and 10 μg L^{-1} but are consistent with previous MART experiments using the same nutrient addition.[46,51,52] After SSA production commenced, the chl *a* concentrations for both experiments decreased below 2 μg L^{-1} within 2 days, remaining below this level for the rest of the experiment. The sharp chl *a* decline is partially caused by the aforementioned damage to fragile phytoplankton cells from the centrifugal pump used for SSA generation, and previous MART studies exhibit this same decline, with chl *a* values dropping to pre-bloom levels in 2–3 days. As a result, most experimental measurements were conducted after the chl *a* maximum. In the open ocean, breaking waves produce SSA during all bloom phases. However, the highest OC enrichment in SSA often occurs after the chl *a* peak, suggesting that the bloom decay phase may be the most important for transfer of "freshly produced" OC into SSA.[46,53,54]

The initial MART1 and MART2 POC concentrations of 46 and 34 μM increased several fold during the experiments to similar maxima of 160 and 151 μM, respectively. Oceanic POC concentrations occasionally reach 100 μM during intense phytoplankton blooms, but the POC concentrations above 150 μM reported here are higher than most open ocean observations.[43] The large POC concentration increase can be

https://dx.doi.org/10.1021/acsearthspacechem.0c00072
ACS Earth Space Chem. 2020, 4, 1686–1699

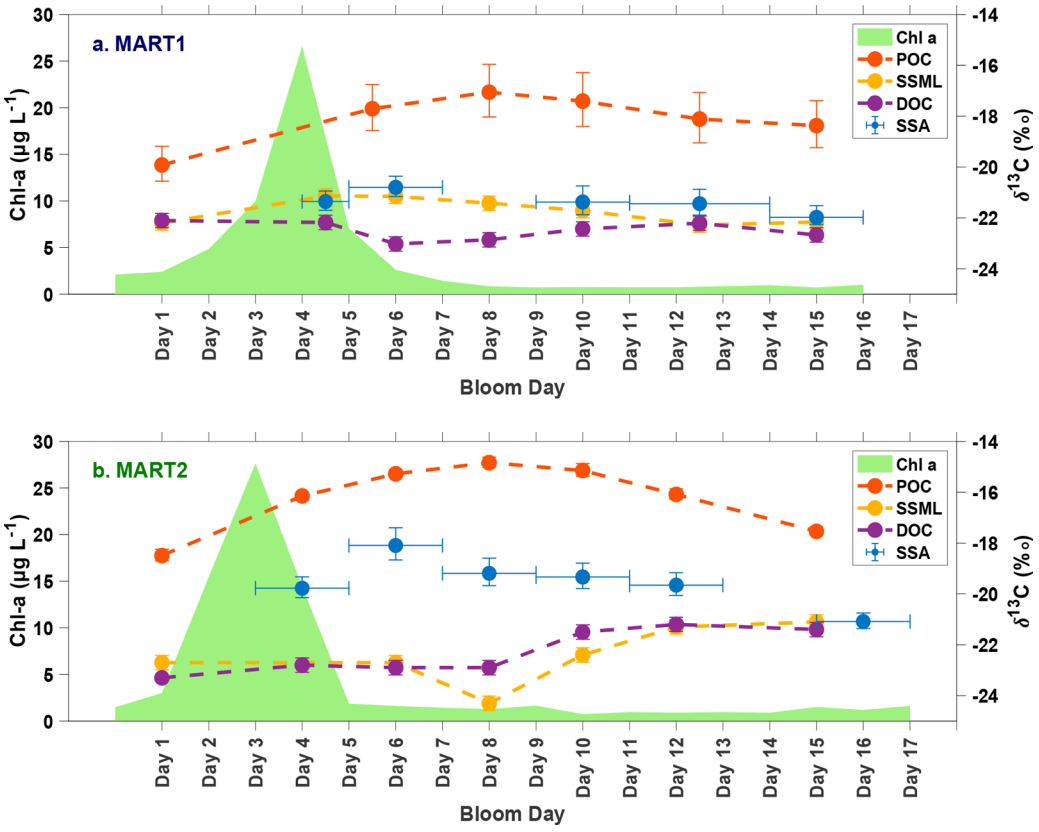

Figure 2. $\delta^{13}C$ values for POC, DOC, SSML, and SSA throughout (a) MART1 and (b) MART2, overlaid on the chl *a* time series. Because SSA was sampled continuously while POC, DOC, and SSML were only measured at individual points, this figure plots the average of two seawater $\delta^{13}C$ values, one at the beginning and end of each SSA collection (Table S1 of the Supporting Information), with the data points in the middle of the collection period (further details in Methods S4 of the Supporting Information). This facilitates an easier comparison between $\delta^{13}C_{SSA}$ and the seawater $\delta^{13}C$ values, showing that $\delta^{13}C_{SSA}$ is consistently less negative than $\delta^{13}C_{DOC}$. Horizontal error bars for SSA indicate the collection duration for each sample, and data points represent the middle of the sampling period. Vertical error bars, calculated as explained in Methods S1 of the Supporting Information, are shown for each species and are approximately the height of the data point for $\delta^{13}C_{DOC}$ and $\delta^{13}C_{SSML}$.

attributed to increased carbon fixation during phytoplankton growth and indicates that the majority of the POC in both experiments is "freshly produced" OC. A decrease in the POC concentration would be expected to accompany the phytoplankton death, as indicated by the chl *a* decline, but the POC concentration was almost the same 2 days after the chl *a* peak in MART2 and had even increased slightly 3 days after the chl *a* peak in MART1. Figure 1 shows that the trends in POC concentrations after the chl *a* maximum in MART1 and MART2 are closely linked to changes in the heterotrophic bacteria concentrations. In both experiments, as chl *a* began declining, heterotrophic bacteria concentrations rose sharply, reaching their maxima 3 and 2 days after the chl *a* peak for MART1 and MART2. The bacteria concentrations showed similar increases of 5−6-fold in both experiments compared to the initial seawater concentrations. The initial seawater bacteria concentrations were higher for MART1 than MART2, which likely explains why bacteria concentrations reached a higher peak in MART1 than MART2. Nevertheless, the maximum concentrations in both experiments were on the order of 10^7 cells mL^{-1}, which is similar to previous MART bloom experiments as well as phytoplankton blooms in the open ocean.[31,46,55,56] When phytoplankton blooms decay, heterotrophic bacteria concentrations often increase when bacteria assimilate "freshly produced" OC, including phytoplankton exudates and detritus.[32,46] The close trend suggests that, after the chl *a* peak, heterotrophic bacteria contribute significantly to POC biomass, implying that a considerable portion of the "freshly produced" OC has undergone bacterial processing.

The initial DOC concentrations were 136 μM for MART1 and 141 μM for MART2, which reached similar maximum values of 218 and 202 μM during both experiments. Accounting for the 12 μM increase from nutrient addition, the DOC concentrations increased by 70 and 49 μM for MART1 and MART2, respectively, compared to the pre-bloom concentrations. These smaller concentration changes indicate that the DOC is mostly comprised of "aged" organic material present in the initial seawater before bloom growth began. Importantly, in comparison to the POC concentration increases of 114 and 117 μM, it is clear that the majority of "freshly produced" OC was in the form of POC for both experiments.

The OC_{SSML} concentrations showed similar trends for both experiments, with the largest OC_{SSML} concentrations, 333 μM for MART1 and 421 μM for MART2, occurring immediately after the chl *a* peak. The OC_{SSML} concentration was higher in MART2 than MART1 following the chl *a* peak, but both decreased to stabilize around 250 μM as the experiments progressed. For both experiments, no measurements of OC_{SSML} were reported for days when room air was being bubbled into the seawater, which included the day of maximum chl *a* concentrations. Although bubbling air into the seawater in the isolated MART is necessary to facilitate phytoplankton growth, this process does not occur in oceanic

https://dx.doi.org/10.1021/acsearthspacechem.0c00072
ACS Earth Space Chem. 2020, 4, 1686−1699

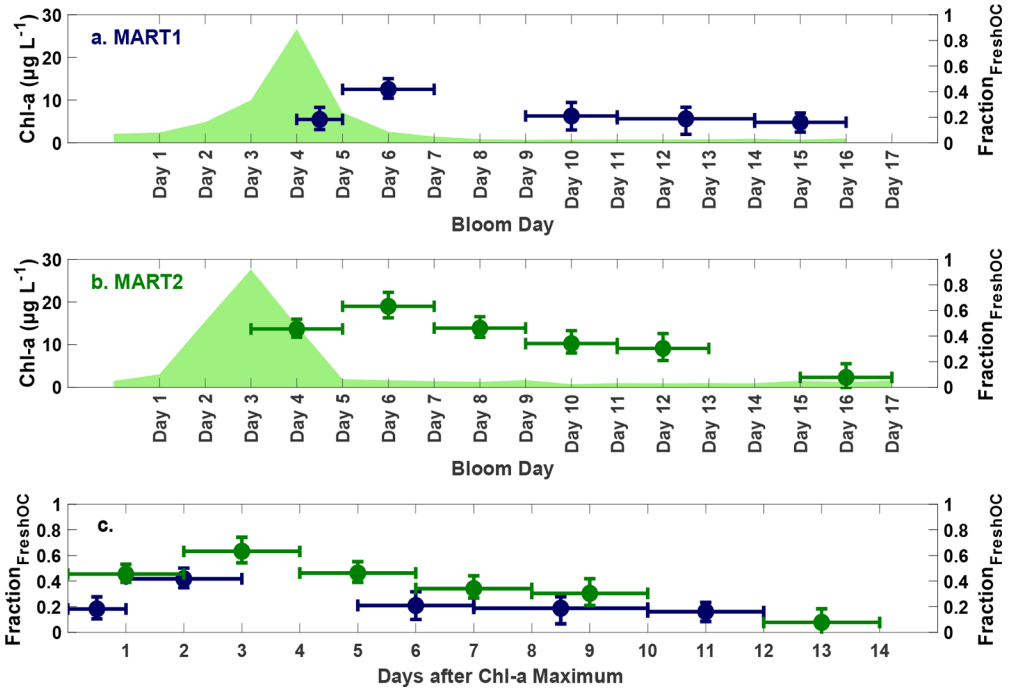

Figure 3. Fractional contribution of "freshly produced" OC to OC_{SSA}, $fraction_{fresh\ OC}$, overlaid on the chl *a* time series for (a) MART1 and (b) MART2. (c) Combined $fraction_{fresh\ OC}$ data from MART1 and MART2 plotted in days after the chl *a* maximum to help facilitate experimental comparison. Both experiments show a similar time lag between the chl *a* maximum and the largest $fraction_{fresh\ OC}$. This time lag, which was 2 days for MART1 and 3 days for MART2, suggests that "freshly produced" OC may undergo bacterial processing before being efficiently transferred into SSA. $Fraction_{fresh\ OC}$ was calculated using eq 2b and the isotopic values from Figure 2 (see Methods S4 of the Supporting Information for more details). Vertical error bars were calculated from the $\delta^{13}C_{SSA}$ uncertainty in Figure 2, and the horizontal error bars represent the collection duration for each SSA sample, with data points placed at the middle of the sampling period.

environments and the air bubbles likely transported organic material to the seawater surface, leading to an overenrichment of organics in the SSML. For this reason, with the exception of day 1 before bubbling was initiated, OC_{SSML} measurements were only reported after the bubbling was stopped and SSA production had commenced.

The OC_{SSA} concentrations for MART1 and MART2 ranged from 3.45 to 5.83 μgC m^{-3} (mean of 4.93 μgC m^{-3}) and 3.86−5.52 μgC m^{-3} (mean of 4.47 μgC m^{-3}), respectively (Figure S2 of the Supporting Information). The higher OC_{SSA} concentrations compared to open ocean measurements reflect higher SSA particle concentrations from the MART, but carbon comprised only 1−2% of TSP SSA mass (Figure S3 of the Supporting Information), comparable to marine observations.[26,57] Similar values for OC_{SSA} concentrations in both experiments is consistent with similar seawater OC concentrations and reproducibility of the SSA generation method.

Seawater $\delta^{13}C$ Constraints on Nascent $\delta^{13}C_{SSA}$ in the Marine Environment. Conducting experiments in an isolated environment enabled the first measurement of $\delta^{13}C_{SSA}$ on nascent SSA without any background aerosol contributions. Figure 2 shows that $\delta^{13}C_{SSA}$ was statistically less negative than the average $\delta^{13}C_{DOC}$ value for each SSA collection period throughout the entirety of both blooms, except for MART2 on days 15−17. This establishes that $\delta^{13}C_{SSA}$ is not necessarily equivalent to $\delta^{13}C_{DOC}$, as has been widely assumed by previous researchers. Interestingly, $\delta^{13}C_{SSA}$ fell between $\delta^{13}C_{POC}$ and $\delta^{13}C_{DOC}$ for the entirety of the MART1 and MART2 experiments, suggesting that the difference between $\delta^{13}C_{SSA}$ and $\delta^{13}C_{DOC}$ can be used to assess the contribution of "freshly produced" OC to OC_{SSA}. This observation is consistent with our earlier hypothesis that OC_{SSA} is comprised of both "freshly produced" and "aged" OC. As described below, validation of this initial hypothesis prompted a more detailed and quantitative examination of how these seawater carbon pools contribute to OC_{SSA} and influence marine $\delta^{13}C_{SSA}$ values.

To estimate the contribution of "freshly produced" OC to OC_{SSA} using the isotopic mixing model introduced in eq 2b, two conditions were mentioned that must be met: (1) $\delta^{13}C_{POC}$ and $\delta^{13}C_{DOC}$ must have isotopically distinct values from one another, and (2) the POC pool should be comprised primarily of "freshly produced" OC, while the DOC pool should be predominantly "aged" OC. As anticipated, increased amounts of isotopically less negative, "freshly produced" OC during the phytoplankton growth phase, most of which was POC, caused $\delta^{13}C_{POC}$ to increase by 3−4‰ in the two experiments (Figure 2). In contrast, $\delta^{13}C_{DOC}$ displayed only modest changes during the phytoplankton growth phase and was distinctly more negative than $\delta^{13}C_{POC}$ throughout both experiments, fulfilling the first condition. With regard to the second condition, as detailed in the "POC−DOC−OC_{SSA} Dynamics during Phytoplankton Blooms" section, the POC and DOC concentrations in Figure 1 show that most POC is "freshly produced" OC, while DOC is primarily "aged" OC. Because the two conditions were satisfied in both experiments, the fractional contribution of "freshly produced" OC to OC_{SSA} for each SSA sample, termed $fraction_{fresh\ OC}$, was calculated and displayed in Figure 3 by approximating that "freshly produced" OC had isotopic values equivalent to $\delta^{13}C_{POC}$ and "aged" OC the same as $\delta^{13}C_{DOC}$.

Figure 3 shows the proportional contribution of "freshly produced" OC to OC_{SSA} necessary to account for the

https://dx.doi.org/10.1021/acsearthspacechem.0c00072
ACS Earth Space Chem. 2020, 4, 1686−1699

difference between $\delta^{13}C_{SSA}$ and $\delta^{13}C_{DOC}$ for each collection. The $fraction_{fresh\ OC}$ values ranged from 7 to 63%, and a contribution of "freshly produced" OC to OC_{SSA} was necessary to explain the measured $\delta^{13}C_{SSA}$ value for every SSA sample in both experiments, demonstrating that OC_{SSA} composition in the marine environment will nominally be comprised of both "freshly produced" and "aged" OC. These findings directly contradict the assertion by some researchers that OC_{SSA} is comprised of only organic species from the "aged" OC pool.[13,22,23] Complementary to the findings in this work, a recent study by Beaupre et al.[58] in the Western Atlantic compared radiocarbon signatures for OC_{SSA} with dissolved inorganic carbon (DIC), a proxy for "freshly produced" OC, and surface DOC, a proxy for "aged" OC. Using their surface DOC measurements as the "aged" end member and surface DIC measurements as the "freshly produced" end member, additional calculations akin to eq 2b indicate that "freshly produced" OC in the Western Atlantic comprises 19−88% of OC_{SSA}. These measurements confirm that "freshly produced" OC is significantly incorporated into OC_{SSA} in the marine environment and show good agreement with the contribution of "freshly produced" OC to SSA observed in this work. Although one might expect that higher amounts of "freshly produced" OC in our nutrient-enhanced biological growth experiments would lead to higher $fraction_{fresh\ OC}$ values, much of this organic material may have been whole phytoplankton and cell detritus too large to be transferred into SSA. Their radiocarbon measurements were conducted on SSA from natural seawater without any stimulated biological growth, suggesting that the $fraction_{fresh\ OC}$ values and OC_{SSA} compositions in our experiments are similar to what would be expected in the natural marine environment.

The radiocarbon measurements showed that the contribution of "freshly produced" OC was largest in coastal regions with elevated chl *a* values, reinforcing the importance of biological activity on OC_{SSA} composition. However, it was also found to be as high as 37% in low biological activity oceanic regimes, suggesting that "freshly produced" OC is a substantial contributor to OC_{SSA} under most oceanic conditions. The authors point out that, while radiocarbon measurements reveal the age of carbon in SSA, $\delta^{13}C$ measurements would have been useful to characterize the sources of carbon contributing to OC_{SSA}. In this study, the $\delta^{13}C$ measurements identified two distinct seawater carbon pools contributing to SSA, with "freshly produced" OC consisting mostly of POC and "aged" OC primarily composed of DOC. Quantifying the incorporation of these two isotopically distinct carbon sources into SSA will improve our understanding of $\delta^{13}C_{SSA}$ variability.

One of the main objectives for this study was to provide better constraints for $\delta^{13}C_{SSA}$ values in the marine environment. The assumption that $\delta^{13}C_{SSA}$ is the same as $\delta^{13}C_{DOC}$ simplified source apportionment studies because most of the "aged" DOC pool has $\delta^{13}C$ values that fall in a narrow range from −20 to −23‰ throughout the surface ocean.[59,60] This work demonstrates in two separate experiments that "freshly produced" OC also contributes substantially to OC_{SSA}. Although the contribution of two separate carbon pools to OC_{SSA} complicates estimates of nascent $\delta^{13}C_{SSA}$, the fact that $\delta^{13}C_{SSA}$ consistently fell between $\delta^{13}C_{POC}$ and $\delta^{13}C_{DOC}$ for both experiments indicates that seawater measurements of $\delta^{13}C_{POC}$ and $\delta^{13}C_{DOC}$ in the marine environment can be used as the upper and lower bounds to constrain the range of potential nascent $\delta^{13}C_{SSA}$ values. In these two experiments, increased biological growth led to $\delta^{13}C_{POC}$ increases of 3−4‰ above the initially measured values, similar to the increases of 3−5‰ for oceanic phytoplankton bloom measurements.[41,42] This resulted in large differences between $\delta^{13}C_{POC}$ and $\delta^{13}C_{DOC}$ of up to 8‰, indicating that oceanic regimes with high biological activity likely lead to less negative values and greater variability in nascent $\delta^{13}C_{SSA}$. Combining the isotopic data for both experiments in Figure 2 provides an expected range of $\delta^{13}C_{SSA}$ values under conditions of high biological activity. The $\delta^{13}C_{SSA}$ values, ranging from −18 to −22‰, have both a wider range and less negative values than the normally assumed range from −20 to −23‰, supporting this assertion. The 1−2‰ increase in TSP $\delta^{13}C_{SSA}$ observed in these experiments agrees well with $\delta^{13}C$ measurements of both submicrometer[34,36] and TSP[61] marine aerosols during high biological activity periods. Although it might be expected that "freshly produced" OC, which is mostly POC (>0.7 μm), would not transfer as efficiently into sub-micrometer SSA, these consistent marine observations imply that "freshly produced" OC may contribute significantly to both submicrometer and TSP SSA during periods of high biological activity. None of the other studies included seawater $\delta^{13}C$ measurements to supplement the aerosol data, but the similarities between their measurements and the results in this work indicate that the less negative $\delta^{13}C_{SSA}$ values in high biological activity regimes are likely applicable to carbon source apportionment studies measuring TSP or sub-micrometer SSA.

Further evidence highlighting the importance of understanding the biological effects on $\delta^{13}C_{SSA}$ is given by comparing the −21‰ value used for previous marine aerosol carbon source apportionment studies[37−39] to the least negative $\delta^{13}C_{SSA}$ value observed in these experiments, −18‰. This seemingly small difference of 3‰ can lead to over a 30% underestimate in the anthropogenic contribution to aerosol carbon in marine environments (Figure S4 of the Supporting Information). These experimental findings indicate that seawater measurements are likely to be especially important in oceanic regimes with high biological activity because the larger difference between $\delta^{13}C_{POC}$ and $\delta^{13}C_{DOC}$ implies a larger range of possible values for $\delta^{13}C_{SSA}$.

It is also pertinent to point out that the majority of the surface ocean has low biological activity levels, and the usual range of $\delta^{13}C_{POC}$ values in low to mid latitudes is from about −18 to −23‰,[62,63] similar to the normal $\delta^{13}C_{DOC}$ range from −20 to −23‰.[59,60] Still, using the $fraction_{fresh\ OC}$ values measured in these two experiments, the gray rectangle in Figure S5 of the Supporting Information shows that the expected range of values for $\delta^{13}C_{SSA}$ in low biological activity regimes is from −18.5 to −23‰ if no $\delta^{13}C_{POC}$ and $\delta^{13}C_{DOC}$ values are measured to provide constraints. These results demonstrate that direct seawater $\delta^{13}C_{DOC}$ and $\delta^{13}C_{POC}$ measurements are extremely valuable for constraining nascent $\delta^{13}C_{SSA}$ values in the marine environment. Incorporating these measurements into future field studies will greatly improve the interpretation of marine aerosol $\delta^{13}C$ values and marine aerosol carbon source apportionments.

Temporal Dependence of "Freshly Produced" OC Contribution to OC_{SSA}. The two isolated MART experiments provide a time series of the biological activity effects on seawater chemistry and nascent OC_{SSA} composition by measuring changes in $\delta^{13}C$. A clear link between oceanic biological activity and OC_{SSA} composition was evident as a

https://dx.doi.org/10.1021/acsearthspacechem.0c00072
ACS Earth Space Chem. 2020, 4, 1686−1699

result of the fact that this study eliminated contributions from the interfering aerosol sources mentioned previously. Most notably, in Figure 3, both experiments exhibit the same temporal trend in $fraction_{fresh\ OC}$, with the highest values delayed from the chl *a* maximum by 2−3 days. Similar results were obtained in a previous MART experiment, where mass spectral organic biomarkers were found to increase in the days following the chl *a* maximum.[46] A time lag between the chl *a* peak and the greatest contribution of "freshly produced" organic material to OC_{SSA} demonstrates that phytoplankton abundance (chl *a*) alone is not sufficient to explain changes in SSA organic enrichment, implying that carbon transfer into SSA is likely influenced by microbial processing in the seawater. Interestingly, Figure S6a of the Supporting Information displaying the OC_{SSA} mass percent for three labile phytoplankton lipid biomarkers in MART1, $C_{16:1}$, $C_{20:5}$, and $C_{22:6}$, shows that the contribution of these labile species to SSA sharply decreases after the first 24 h. Although the MART2 SSA sample collected for the first 48 h after the chl *a* peak was not available for lipid measurements, Figure S6b of the Supporting Information similarly shows that the OC_{SSA} contribution of these labile lipid biomarkers is low for samples collected more than 48 h after the chl *a* peak. Consistent with these measurements, a recent phytoplankton bloom mesocosm experiment found that enrichment of highly labile, aliphatic organic matter in SSA was highest during the chl *a* peak, and this enrichment mostly disappeared within 24 h after the chl *a* maximum.[32] This was attributed to rapid bacterial enzymatic degradation of highly labile organic matter in the seawater, revealing that seawater bacterial activity, in addition to phytoplankton abundance, controls enrichment of organic matter in SSA. This study extends the previous research on SSA organic enrichment by demonstrating that, while the contribution of highly labile organic species to SSA may be highest immediately following the chl *a* peak, the largest proportional contribution of "freshly produced" OC to SSA is delayed from the chl *a* maximum by 2−3 days. These findings suggest that the highest enrichment of "freshly produced" OC in SSA occurs after this organic material has been partially degraded by bacteria and imply that bacterial processing may lead to more efficient transfer of "freshly produced" organic material into SSA.

Similar to the findings in this work, Rinaldi et al.[56] have observed that a time lag of 5−7 days, accounting for the air mass travel time, gives the highest correlation between chl *a* and the contribution of water-insoluble organic matter (WIOM) to sub-micrometer SSA in ocean waters with high chl *a* concentrations. The authors hypothesized that this time lag might be due to seawater biological processes producing organic material that is more efficiently transferred into SSA but did not directly resolve the relationship between increased WIOM enrichment in SSA and biological processes occurring in the seawater. Their field observations align well with our bloom experiments, where an increased proportional contribution of more insoluble, "freshly produced" OC to OC_{SSA} occurred 2−3 days delayed from the maximum chl *a* concentration. Because most of the "freshly produced" organic material formed during phytoplankton growth was in the POC pool, the time lag is likely related to the degradation of "freshly produced" POC into sizes small enough to efficiently transfer into SSA. In this study, "freshly produced" organic material during the phytoplankton growth phase, as indicated by chl *a*, is likely dominated by whole, living phytoplankton, many of which are >10 μm in diameter,[64] larger than the majority of SSA particles (Figure S1a of the Supporting Information). Immediately following the chl *a* peak in both experiments, the heterotrophic bacteria concentration swiftly increased, resulting in the breakdown of "freshly produced" organic material into smaller phytoplankton exudates and detritus as well as organic aggregates. For both MART1 and MART2, bacterial abundance was highest either during or before the SSA sampling period with the largest $fraction_{fresh\ OC}$, suggesting that several days after the chl *a* maximum bacterial processing may have degraded "freshly produced" OC into small enough sizes to be more effectively enriched in SSA. The proposed mechanism is supported by bubbling experiments on biologically active seawater that showed that the ^{1}H NMR spectra of sub-micrometer marine aerosol closely match the spectra for POC of <10 μm.[22] This would also explain why the observed time lag was longer for sub-micrometer SSA compared to this study on TSP SSA, because the "freshly produced" OC would need to be broken down into smaller sizes to be transferred into the sub-micrometer aerosols. Although the exact physicochemical mechanisms controlling the breakdown of "freshly produced" OC and enrichment in SSA cannot be fully resolved by these isotopic measurements, the comparable time lag between peak chl *a* and maximum "freshly produced" OC contribution to OC_{SSA} for both MART experiments strongly points to the important role heterotrophic bacteria play in controlling carbon transfer during separate phytoplankton blooms. The isotopic measurements highlight the influence of seawater microbiology on SSA carbon transfer and composition, confirming conclusions from previous research indicating that this influence depends upon both phytoplankton and bacterial abundance. These insights into the chemical and biological factors controlling carbon transfer and OC_{SSA} composition are important for parametrizing SSA hygroscopic growth factors and light scattering, linking differences in OC_{SSA} composition with climate-relevant SSA properties.

Impact of Seawater Carbon Pools on Variability in $\delta^{13}C_{SSA}$ and $fraction_{fresh\ OC}$. Although $\delta^{13}C_{SSA}$ was consistently higher than $\delta^{13}C_{DOC}$ in both experiments, the difference between these two values appears to be more pronounced for MART2, where $\delta^{13}C_{SSA}$ values ranged from −18 to −21‰, with most measurements falling outside the typically assumed values from −20 to −23‰. Conversely, $\delta^{13}C_{SSA}$ values for MART1, from −20 to −22‰, remained within the normally assumed range. A portion of the difference in $\delta^{13}C_{SSA}$ values for these experiments can be explained by the higher initial seawater $\delta^{13}C_{POC}$ value of −18.5‰ in MART2 compared to −20‰ in MART1. Both of these values fall within the typical $\delta^{13}C_{POC}$ ranges observed in the surface ocean,[62,63] and the initial seawater for the two experiments was collected from the same location using an identical procedure, suggesting that the differences are simply due to variability in $\delta^{13}C_{POC}$ at this location on the two separate collection dates. With the application of the same $\delta^{13}C_{DOC}$ and $fraction_{fresh\ OC}$ values observed in MART2, if the initial seawater $\delta^{13}C_{POC}$ had been −20‰ instead of −18.5‰, eq 2a indicates that the $\delta^{13}C_{SSA}$ range in MART2 would have been up to 1‰ more negative, from −19 to −21‰. This reinforces our previous assertion that seawater measurements of $\delta^{13}C_{POC}$ and $\delta^{13}C_{DOC}$ will help constrain $\delta^{13}C_{SSA}$ variability in the marine environment.

The other reason for less negative $\delta^{13}C_{SSA}$ values in MART2 is shown in Figure 3, where, despite similar temporal trends, MART2 generally exhibited larger $fraction_{fresh\ OC}$ values than

https://dx.doi.org/10.1021/acsearthspacechem.0c00072
ACS Earth Space Chem. 2020, 4, 1686−1699

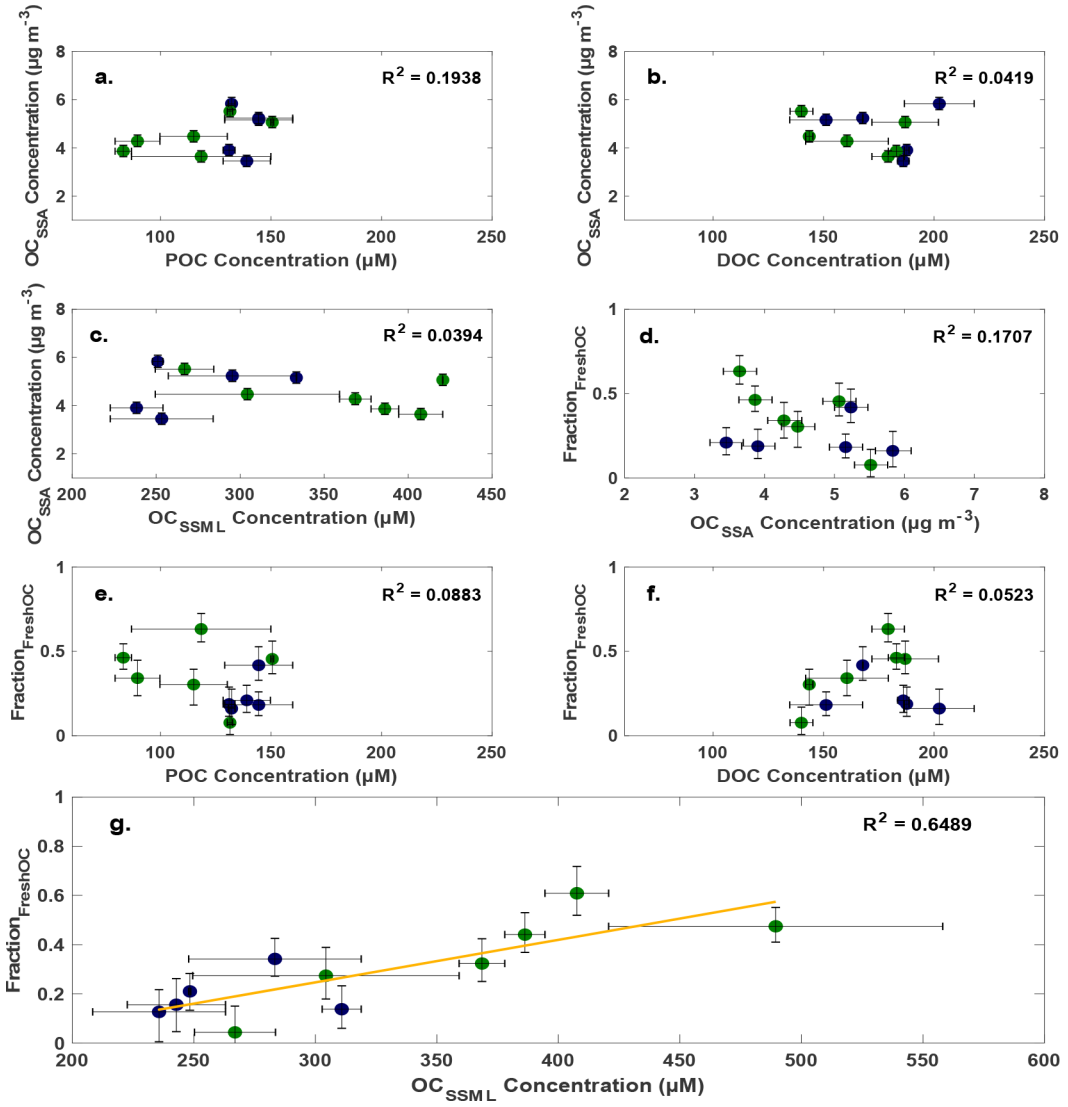

Figure 4. Correlation scatter plots of (a) POC, (b) DOC, and (c) OC_{SSML} with OC_{SSA}, (d) OC_{SSA} with $fraction_{fresh\ OC}$, and (e) POC, (f) DOC, and (g) OC_{SSML} with $fraction_{fresh\ OC}$ for the combined data from MART1 (dark blue dots) and MART2 (green dots). The only significant correlation was between the OC_{SSML} concentration and $fraction_{fresh\ OC}$ (g), with higher OC_{SSML} concentrations leading to the increased proportional transfer of "freshly produced" OC into SSA. Vertical error bars are included for all data points, and horizontal error bars represent the likely range of concentrations during each SSA collection period.

MART1, suggesting a greater contribution of "freshly produced" OC to SSA for MART2. To investigate potential factors impacting the contribution of "freshly produced" OC to OC_{SSA}, correlation plots were made for the combined data from MART1 and MART2 to compare changes in POC, DOC, and OC_{SSML} concentrations to changes in the OC_{SSA} concentration and $fraction_{fresh\ OC}$ (Figure 4). The only significant correlation for the combined experiments, R^2 = 0.6489, was between the OC_{SSML} concentration and $fraction_{fresh\ OC}$ (Figure 4g), where higher OC_{SSML} concentrations corresponded to a larger $fraction_{fresh\ OC}$ in SSA. One plausible explanation would be that the SSML contained more "freshly produced" OC and higher OC_{SSML} concentrations resulted in a larger contribution of this carbon pool to SSA. However, if OC_{SSML} was contributing more to OC_{SSA}, one would expect that their chemical composition and, thus, $\delta^{13}C_{SSML}$ and $\delta^{13}C_{SSA}$ values should be similar. Figure 2b shows that the two SSA samples with the highest $fraction_{fresh\ OC}$ values and least negative $\delta^{13}C_{SSA}$ values, MART2 on Days 6–8 and 8–10, correspond to the most negative $\delta^{13}C_{SSML}$ values. This indicates that, on these days, the OC_{SSA} chemical composition was actually not similar to the OC_{SSML} composition. Moreover, Figure 4c displays no correlation between OC_{SSML} and OC_{SSA} concentrations, suggesting that increased OC_{SSML} concentrations did not lead to larger amounts of carbon transferred into SSA but only to an increased proportional contribution of "freshly produced" OC to SSA. Because changes in seawater chemical composition do not seem to fully account for the differences in $fraction_{fresh\ OC}$ between MART1 and MART2, we speculate below on two complementary explanations that address the primary formation mechanisms for SSA in the context of the relationship between higher OC_{SSML} concentrations and a higher contribution of "freshly produced" OC to SSA. These explanations are consistent with our measurements and recent research regarding the physical processes that affect carbon transfer into SSA.

https://dx.doi.org/10.1021/acsearthspacechem.0c00072
ACS Earth Space Chem. 2020, 4, 1686−1699

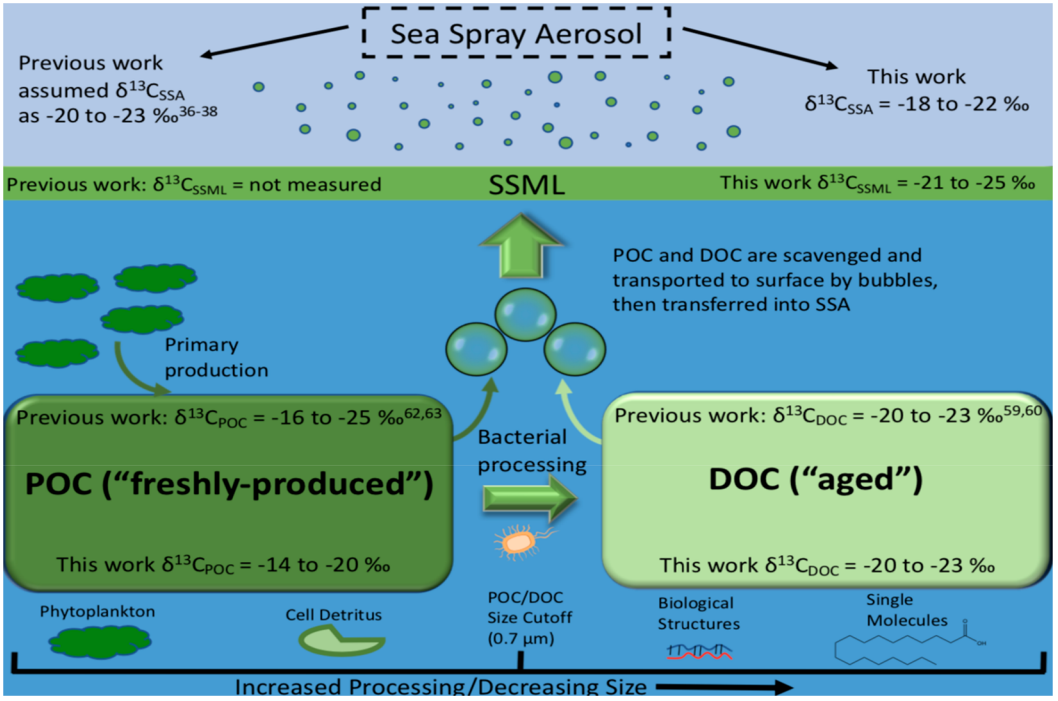

Figure 5. Schematic depicting the relationship between the different seawater carbon pools and their transfer processes into SSA. POC formed by primary production can be converted to DOC by microbial processing, and both POC and DOC are scavenged by bubbles, brought to the SSML, and subsequently enriched in SSA. The size spectrum at the bottom of the schematic shows typical organisms and molecules in the seawater along with the operational 0.7 μm size cutoff used in this work for POC and DOC. Also included are the $\delta^{13}C_{POC}$, $\delta^{13}C_{DOC}$, $\delta^{13}C_{SSML}$, and $\delta^{13}C_{SSA}$ ranges from this work observed during periods of high biological activity as well as open ocean values from previous works (with references) for comparison.

Recent bubble-bursting experiments by Chingin et al.[65,66] indicate that adsorption of organics to the bubble surface begins as a kinetic process immediately following bubble formation but transitions into a competitive equilibrium process as the bubble rises through the water column and its surface becomes saturated with organics. The competitive equilibrium process favors more aliphatic, insoluble organic species (e.g., lipids and biomolecules), which have a higher affinity for the bubble surface. Their research shows that, for the seawater OC concentrations around 300 μM and bubble rise paths around 25 cm in our MART experiments, many bubbles will likely be saturated with organics before reaching the SSML. Because the bubble surface will already be saturated by the time the bubble rises to the SSML, the only way organic species near the seawater surface can be transferred to the bubble surface is through competitive equilibrium adsorption, which favors more aliphatic, insoluble "freshly produced" OC. Previous bubble-bursting studies have found that higher OC concentrations in surface seawater lead to bubble stabilization, increasing bubble residence time at the air−sea interface and allowing for more equilibrium adsorption.[67,68]

Super-micrometer SSA is primarily comprised of jet drops, which form from bulk seawater below the SSML;[15] therefore, their chemical composition is not expected to reflect the composition of the SSML. This super-micrometer SSA still includes organic material from the base of the bubble; therefore, the competitive equilibrium adsorption could lead to an increased proportion of "freshly produced" OC in super-micrometer SSA. An increased proportion of "freshly produced" OC in super-micrometer SSA would explain why the $\text{fraction}_{\text{fresh OC}}$ increases but the OC_{SSA} chemical composition is not similar to the OC_{SSML}. On the other hand, sub-micrometer SSA are mostly formed from the bubble film when the bubble bursts. Longer bubble residence at the air−sea interface has been found to increase drainage of more soluble, "aged" OC from the bubble film back into the seawater, resulting in a larger proportion of "freshly produced" OC remaining on the bubble surface before bursting to form SSA.[69] This provides a rationale for how the proportion of "freshly produced" OC could be higher in sub-micrometer SSA at higher OC_{SSML} concentrations.

These two MART experiments highlight the important influence of the SSML on carbon transfer and OC_{SSA} chemical composition and suggest that more comprehensive concentration and chemical composition measurements of the SSML during field studies may be useful to characterize OC_{SSA} chemical composition in the marine environment. Additionally, while our isotopic data cannot definitively establish that changes in bubble dynamics directly affected the contribution of "freshly produced" OC to SSA, future research focusing on the potentially significant impact of bubble persistence and drainage as well as size dependence of OC_{SSA} composition could be important to elucidate the fundamental mechanisms controlling carbon transfer into SSA.

CONCLUSIONS AND ATMOSPHERIC IMPLICATIONS

This study performed two phytoplankton blooms in a highly characterized laboratory environment to evaluate the $\delta^{13}C$ value of isolated, nascent SSA and examine how $\delta^{13}C_{SSA}$ is influenced by seawater biological activity. The two phytoplankton bloom experiments revealed that $\delta^{13}C_{SSA}$ is consistently less negative than $\delta^{13}C_{DOC}$ during high biological activity regimes (Figure 2) because of a significant contribution

https://dx.doi.org/10.1021/acsearthspacechem.0c00072
ACS Earth Space Chem. 2020, 4, 1686−1699

of isotopically less negative "freshly produced" OC to OC_{SSA}. Figure 5 depicts a simplified representation of how biological activity affects the seawater POC and DOC pools and shows the processes by which these carbon pools influence OC_{SSA} composition. The range of $\delta^{13}C$ values observed in the high biological activity regimes from this work are presented in Figure 5 for POC, DOC, SSML, and SSA. Some open ocean $\delta^{13}C$ measurements made over a wider range of biological activity levels are included from previous studies for comparison. To our knowledge, this work provides the first $\delta^{13}C_{SSML}$ measurements for a non-polluted sea surface and the first measurements for pure, nascent $\delta^{13}C_{SSA}$.

In addition to characterizing the effects of seawater chemical composition and microbiology on $\delta^{13}C_{SSA}$, these laboratory bloom experiments enabled nascent $\delta^{13}C_{SSA}$ measurements before any atmospheric aging occurred. This has important implications for the OC_{SSA} composition and $\delta^{13}C$ values observed in this study compared to marine aerosols. Chemical aging can lead to the formation of marine SOA, which is believed to have a more negative $\delta^{13}C$ value than primary SSA; therefore, source apportionment studies will need to account for the contribution of marine SOA to total marine aerosol carbon before applying the $\delta^{13}C_{SSA}$ values measured in these experiments.[69−71] Dual-isotopic mixing is only able to distinguish between marine and terrestrial aerosol contributions, but atmospheric source apportionment studies would benefit greatly from the ability to separate primary and secondary marine aerosol carbon. These two experiments provide constraints on the $\delta^{13}C$ values for primary SSA, and applying these values to marine aerosols in the remote marine environment (with minimal terrestrial contributions) can help future atmospheric studies differentiate between primary and secondary marine aerosols.

Additionally, aging of primary OC_{SSA} often leads to $\delta^{13}C$ increases during atmospheric transport.[71−74] Dasari et al.[74] have used the isotopic shift between source and receptor sites as a proxy to model the extent of aerosol aging. Field studies often collect SSA from air masses that have been traveling several days; therefore, this study provides an isotopic source characterization of nascent SSA that can be integrated with marine measurements to evaluate aging of SSA. Aerosol aging can cause climatically significant changes in absorptivity and hygroscopicity;[73−76] therefore, measuring $\delta^{13}C$ for nascent, unaltered SSA provides a critical reference point to understand the impact of aging on climatically relevant SSA properties.

Up to this point, many marine field studies have focused on simple measurements of OC_{SSA} concentrations and enrichment factors to characterize SSA carbon. This is understandable because identification of unaltered, "freshly produced" organic species is complicated by rapid degradation of this highly labile organic material in the ocean and photochemical alteration during atmospheric transport. Nevertheless, it is highly recommended that future field studies supplement bulk OC_{SSA} measurements by including direct measurements of chemical or isotopic composition for seawater POC, seawater DOC, OC_{SSML}, and OC_{SSA} to address the transfer of "freshly produced" OC into SSA. Our isotopic measurements indicate that the most significant biological influence on OC_{SSA} occurred 2−3 days after the chl *a* peak and suggest that the contribution of "freshly produced" OC to OC_{SSA} is strongly dependent upon the degradation processes and time scales for incorporation of this organic material into nascent SSA as it forms at the ocean surface. These findings imply that accurate knowledge of seawater enzymatic activity and kinetics for microbial degradation of "freshly produced" organic material is integral to understand biological impacts on OC_{SSA} composition, and measurements of these properties should be a focus of future marine field studies.

■ ASSOCIATED CONTENT

Supporting Information

The Supporting Information is available free of charge at https://pubs.acs.org/doi/10.1021/acsearthspacechem.0c00072.

Description of measurement uncertainties and filter blank analyses (Methods S1), description of total SSA mass and carbon mass percent calculations (Methods S2), description of lipid analysis and contribution to SSA (Methods S3), description of $fraction_{fresh\ OC}$ calculations and correlation plots for seawater OC and SSA (Methods S4), aerosol size and mass distributions during MART2 (Figure S1), OC_{SSA} concentrations for MART1 and MART2 (Figure S2), OC_{SSA} mass percent for MART1 and MART2 (Figure S3), concentration and isotope values for MART1 and MART2 (Table S1), importance of the $\delta^{13}C_{SSA}$ value to marine aerosol carbon source apportionments (Figure S4), potential $\delta^{13}C_{SSA}$ range for low biological activity waters (Figure S5), and OC_{SSA} mass percent for $C_{16:1}$, $C_{20:5}$, and $C_{22:6}$ lipid biomarkers in MART1 and MART2 SSA samples (Figure S6) (PDF)

■ AUTHOR INFORMATION

Corresponding Authors

Kimberly A. Prather − *Department of Chemistry and Biochemistry and Scripps Institution of Oceanography, University of California, San Diego, La Jolla, California 92093, United States*; Phone: 858-822-5312; Email: kprather@ucsd.edu

Mark H. Thiemens − *Department of Chemistry and Biochemistry, University of California, San Diego, La Jolla, California 92093, United States*; Phone: 858-534-6053; Email: mthiemens@ucsd.edu

Authors

Daniel R. Crocker − *Department of Chemistry and Biochemistry, University of California, San Diego, La Jolla, California 92093, United States*; orcid.org/0000-0002-5297-1103

Ritchie E. Hernandez − *Department of Chemistry and Biochemistry, University of California, San Diego, La Jolla, California 92093, United States*

Haonan D. Huang − *Department of Chemistry and Biochemistry, University of California, San Diego, La Jolla, California 92093, United States*

Matthew A. Pendergraft − *Scripps Institution of Oceanography, University of California, San Diego, La Jolla, California 92093, United States*

Ruochen Cao − *Department of Chemistry and Biochemistry, University of California, San Diego, La Jolla, California 92093, United States*

Jiayin Dai − *Department of Chemistry and Biochemistry, University of California, San Diego, La Jolla, California 92093, United States*

https://dx.doi.org/10.1021/acsearthspacechem.0c00072
ACS Earth Space Chem. 2020, 4, 1686−1699

Clare K. Morris − *Scripps Institution of Oceanography, University of California, San Diego, La Jolla, California 92093, United States*

Grant B. Deane − *Scripps Institution of Oceanography, University of California, San Diego, La Jolla, California 92093, United States*

Complete contact information is available at: https://pubs.acs.org/10.1021/acsearthspacechem.0c00072

Notes

The authors declare no competing financial interest.

■ ACKNOWLEDGMENTS

This material is based on work supported by the National Science Foundation through the Centers for Chemical Innovation Program under Grant CHE-1801971. The authors thank Kathryn Mayer for assistance with aerosol sizing measurements and Bruce Deck for assistance with POC isotope measurements. The authors also thank Subrata Chakraborty, Lihini Aluwihare, Francesca Malfatti, and Nicole Peiris for helpful discussions.

■ REFERENCES

(1) Quinn, P. K.; Collins, D. B.; Grassian, V. H.; Prather, K. A.; Bates, T. S. Chemistry and Related Properties of Freshly Emitted Sea Spray Aerosol. *Chem. Rev.* **2015**, *115* (10), 4383−4399.

(2) de Leeuw, G.; Andreas, E. L.; Anguelova, M. D.; Fairall, C. W.; Lewis, E. R.; O'Dowd, C.; Schulz, M.; Schwartz, S. E. Production flux of sea spray aerosol. *Rev. Geophys.* **2011**, *49*, RG2001.

(3) Prather, K. A.; Bertram, T. H.; Grassian, V. H.; Deane, G. B.; Stokes, D. M.; DeMott, P. J.; Aluwihare, L. I.; Palenik, B. P.; Azam, F.; Seinfeld, J. H.; Moffet, R. C.; Molina, M. J.; Cappa, C. D.; Geiger, F. M.; Roberts, G. C.; Russell, L. M.; Ault, A. P.; Baltrusaitis, J.; Collins, D. B.; Corrigan, C. E.; Cuadra-Rodriguez, L. A.; Ebben, C. J.; Forestieri, S. D.; Guasco, T. L.; Hersey, S. P.; Kim, M. J.; Lambert, W. F.; Modini, R. L.; Mui, Wilton; Pedler, B. E.; Ruppel, M. J.; Ryder, O. S.; Schoepp, N. G.; Sullivan, R. C.; Zhao, D. Bringing the ocean into the laboratory to probe the chemical complexity of sea spray aerosol. *Proc. Natl. Acad. Sci. U. S. A.* **2013**, *110* (19), 7550−7555.

(4) Bertram, T. H.; Cochran, R. E.; Grassian, V. H.; Stone, E. A. Sea spray aerosol chemical composition: Elemental and molecular mimics for laboratory studies of heterogeneous and multiphase reactions. *Chem. Soc. Rev.* **2018**, *47* (7), 2374−2400.

(5) Ovadnevaite, J.; O'Dowd, C.; Dall'Osto, M.; Ceburnis, D.; Worsnop, D. R.; Berresheim, H. Detecting high contributions of primary organic matter to marine aerosol: A case study. *Geophys. Res. Lett.* **2011**, *38* (2), L02807.

(6) Patterson, J. P.; Collins, D. B.; Michaud, J. M.; Axson, J. L.; Sultana, C. M.; Moser, T.; Dommer, A. C.; Conner, J.; Grassian, V. H.; Stokes, M. D.; Deane, G. B.; Evans, J. E.; Burkart, M. D.; Prather, K. A.; Gianneschi, N. C. Sea Spray Aerosol Structure and Composition Using Cryogenic Transmission Electron Microscopy. *ACS Cent. Sci.* **2016**, *2* (1), 40−47. Schmitt-Kopplin, P.; Liger-Belair, G.; Koch, B. P.; Flerus, R.; Kattner, G.; Harir, M.; Kanawati, B.; Lucio, M.; Tziotis, D.; Hertkorn, N.; Gebefügi, I. Dissolved organic matter in sea spray: A transfer study from marine surface water to aerosols. *Biogeosciences* **2012**, *9*, 1571−1582.

(7) Boucher, O.; Randall, D.; Artaxo, P.; Bretherton, C.; Feingold, G.; Forster, P.; Kerminen, V.-M.; Kondo, Y.; Liao, H.; Lohmann, U.; Rasch, P.; Satheesh, S. K.; Sherwood, S.; Stevens, B.; Zhang, X. Y. Clouds and Aerosols. *Climate Change 2013: The Physical Science Basis. Contribution of Working Group I to the Fifth Assessment Report of the Intergovernmental Panel on Climate Change*; Cambridge University Press: New York, 2013.

(8) Keene, W. C.; Maring, H.; Maben, J. R.; Kieber, D. J.; Pszenny, A. A.; Dahl, E. E.; Izaguirre, M. A.; Davis, A. J.; Long, M. S.; Zhou, X.; Smoydzin, L.; Sander, R. Chemical and physical characteristics of nascent aerosols produced by bursting bubbles at a model air-sea interface. *J. Geophys. Res.* **2007**, *112*, D21202.

(9) Sellegri, K.; O'Dowd, C. D.; Yoon, Y. J.; Jennings, S. G.; de Leeuw, G. Surfactants and submicron sea spray generation. *J. Geophys. Res.* **2006**, *111*, D22215.

(10) Forestieri, S. D.; Cornwell, G. C.; Helgestad, T. M.; Moore, K. A.; Lee, C.; Novak, G. A.; Sultana, C. M.; Wang, X.; Bertram, T. H.; Prather, K. A.; Cappa, C. D. Linking variations in sea spray aerosol particle hygroscopicity to composition during two microcosm experiments. *Atmos. Chem. Phys.* **2016**, *16*, 9003−9018.

(11) DeMott, P. J.; Hill, T. C. J.; McCluskey, C. S.; Prather, K. A.; Collins, D. B.; Sullivan, R. C.; Ruppel, M. J.; Mason, R. H.; Irish, V. E.; Lee, T.; Hwang, C. Y.; Rhee, T. S.; Snider, J. R.; McMeeking, G. R.; Dhaniyala, S.; Lewis, E. R.; Wentzell, J. J. B.; Abbatt, J.; Lee, C.; Sultana, C. M.; Ault, A. P.; Axson, J. L.; Diaz Martinez, M.; Venero, I.; Santos-Figueroa, G.; Stokes, M. D.; Deane, G. B.; Mayol-Bracero, A. L.; Grassian, V. H.; Bertram, T. H.; Bertram, A. K.; Moffett, B. F.; Franc, G. D. Sea spray aerosol as a unique source of ice nucleating particles. *Proc. Natl. Acad. Sci. U. S. A.* **2016**, *113* (21), 5797−5803.

(12) Schmitt-Kopplin, P.; Liger-Belair, G.; Koch, B. P.; Flerus, R.; Kattner, G.; Harir, M.; Kanawati, B.; Lucio, M.; Tziotis, D.; Hertkorn, N.; Gebefügi, I. Dissolved organic matter in sea spray: A transfer study from marine surface water to aerosols. *Biogeosciences* **2012**, *9*, 1571−1582.

(13) Quinn, P. K.; Bates, T. S.; Schulz, K. S.; Coffman, D. J.; Frossard, A. A.; Russell, L. M.; Keene, W. C.; Kieber, D. J. Contribution of sea surface carbon pool to organic matter enrichment in sea spray aerosol. *Nat. Geosci.* **2014**, *7* (3), 228−232.

(14) Blanchard, D. C. Sea-to-Air Transport of Surface Active Material. *Science* **1964**, *146* (3642), 396−397.

(15) Wang, X.; Deane, G. B.; Moore, K. A.; Ryder, O. S.; Stokes, M. D.; Beall, C. M.; Collins, D. B.; Santander, M. S.; Burrows, S. M.; Sultana, C. M.; Prather, K. A. The role of jet and film drops in controlling the mixing state of submicron sea spray aerosol particles. *Proc. Natl. Acad. Sci. U. S. A.* **2017**, *114* (27), 6978−6983.

(16) van Pinxteren, M.; Müller, C.; Iinuma, Y.; Stolle, C.; Herrmann, H. Chemical Characterization of Dissolved Organic Compounds from Coastal Sea Surface Microlayers (Baltic Sea, Germany). *Environ. Sci. Technol.* **2012**, *46* (19), 10455−10462.

(17) Cunliffe, M.; Engel, A.; Frka, S.; Gašparović, B.; Guitart, C.; Murrell, J. C.; Salter, M.; Stolle, C.; Upstill-Goddard, R.; Wurl, O. Sea surface microlayers: A unified physicochemical and biological perspective of the air−ocean interface. *Prog. Oceanogr.* **2013**, *109*, 104−116.

(18) Wurl, O.; Wurl, E.; Miller, L.; Johnson, K.; Vagle, S. Formation and global distribution of sea-surface microlayers. *Biogeosciences* **2011**, *8* (1), 121−135.

(19) Bates, T. S.; Quinn, P. K.; Coffman, D. J.; Johnson, J. E.; Upchurch, L.; Saliba, G.; Lewis, S.; Graff, J.; Russell, L. M.; Behrenfeld, M. J. Variability in Marine Plankton Ecosystems Are Not Observed in Freshly Emitted Sea Spray Aerosol Over the North Atlantic Ocean. *Geophys. Res. Lett.* **2020**, *47* (1), e2019GL085938.

(20) Kieber, D. J.; Keene, W. C.; Frossard, A. A.; Long, M. S.; Maben, J. R.; Russell, L. M.; Kinsey, J. D.; Tyssebotn, I. M. B.; Quinn, P. K.; Bates, T. S. Coupled ocean-atmosphere loss of marine refractory dissolved organic carbon. *Geophys. Res. Lett.* **2016**, *43* (6), 2765−2772.

(21) O'Dowd, C. D.; Facchini, M. C.; Cavalli, F.; Ceburnis, D.; Mircea, M.; Decesari, S.; Fuzzi, S.; Yoon, Y. J.; Putaud, J. Biogenically driven organic contribution to marine aerosol. *Nature* **2004**, *431* (7009), 676−680.

(22) Facchini, M. C.; Rinaldi, M.; Decesari, S.; Carbone, C.; Finessi, E.; Mircea, M.; Fuzzi, S.; Ceburnis, D.; Flanagan, R.; Nilsson, E. D.; de Leeuw, G.; Martino, M.; Woeltjen, J.; O'Dowd, C. D. Primary submicron marine aerosol dominated by insoluble organic colloids and aggregates. *Geophys. Res. Lett.* **2008**, *35*, L17814.

(23) Cavalli, F.; Facchini, M. C.; Decesari, S.; Mircea, M.; Emblico, L.; Fuzzi, S.; Ceburnis, D.; Yoon, Y. J.; O'Dowd, C. D.; Putaud, J. P.;

Dell'Acqua, A. Advances in characterization of size-resolved organic matter in marine aerosol over the North Atlantic. *J. Geophys. Res.* **2004**, *109*, D24215.
(24) Yoon, Y. J.; Ceburnis, D.; Cavalli, F.; Jourdan, O.; Putaud, J. P.; Facchini, M. C.; Decesari, S.; Fuzzi, S.; Sellegri, K.; Jennings, S. G.; O'Dowd, C. D. Seasonal characteristics of the physicochemical properties of North Atlantic marine atmospheric aerosols. *J. Geophys. Res.* **2007**, *112* (D4), D04206.
(25) Pomeroy, L.; Williams, P. J. L.; Azam, F.; Hobbie, J. The Microbial Loop. *Oceanography* **2007**, *20* (2), 28−33.
(26) Smith, D. C.; Simon, M.; Alldredge, A. L.; Azam, F. Intense hydrolytic enzyme activity on marine aggregates and implications for rapid particle dissolution. *Nature* **1992**, *359* (6391), 139−142.
(27) Tremblay, L.; Caparros, J.; Leblanc, K.; Obernosterer, I. Origin and fate of particulate and dissolved organic matter in a naturally iron-fertilized region of the Southern Ocean. *Biogeosciences* **2015**, *12* (2), 607−621.
(28) Cochran, R. E.; Laskina, O.; Jayarathne, T.; Laskin, A.; Laskin, J.; Lin, P.; Sultana, C.; Lee, C.; Moore, K. A.; Cappa, C. D.; Bertram, T. H.; Prather, K. A.; Grassian, V. H.; Stone, E. A. Analysis of Organic Anionic Surfactants in Fine and Coarse Fractions of Freshly Emitted Sea Spray Aerosol. *Environ. Sci. Technol.* **2016**, *50* (5), 2477−2486.
(29) Shank, L. M.; Howell, S.; Clarke, A. D.; Freitag, S.; Brekhovskikh, V.; Kapustin, V.; McNaughton, C.; Campos, T.; Wood, R. Organic matter and non-refractory aerosol over the remote Southeast Pacific: Oceanic and combustion sources. *Atmos. Chem. Phys.* **2012**, *12* (1), 557−576.
(30) Gantt, B.; Meskhidze, N. The physical and chemical characteristics of marine primary organic aerosol: A review. *Atmos. Chem. Phys.* **2013**, *13* (8), 3979−3996.
(31) Malfatti, F.; Lee, C.; Tinta, T.; Pendergraft, M. A.; Celussi, M.; Zhou, Y.; Sultana, C. M.; Rotter, A.; Axson, J. L.; Collins, D. B.; Santander, M. V.; Anides Morales, A. L.; Aluwihare, L. I.; Riemer, N.; Grassian, V. H.; Azam, F.; Prather, K. A. Detection of Active Microbial Enzymes in Nascent Sea Spray Aerosol: Implications for Atmospheric Chemistry and Climate. *Environ. Sci. Technol. Lett.* **2019**, *6* (3), 171−177.
(32) Wang, X.; Sultana, C. M.; Trueblood, J.; Hill, T. C.; Malfatti, F.; Lee, C.; Laskina, O.; Moore, K. A.; Beall, C. M.; McCluskey, C. S.; Cornwell, G. C.; Zhou, Y.; Cox, J. L.; Pendergraft, M. A.; Santander, M. V.; Bertram, T. H.; Cappa, C. D.; Azam, F.; DeMott, P. J.; Grassian, V. H.; Prather, K. A. Microbial Control of Sea Spray Aerosol Composition: A Tale of Two Blooms. *ACS Cent. Sci.* **2015**, *1* (3), 124−131.
(33) Kundu, S.; Kawamura, K. Seasonal variations of stable carbon isotopic composition of bulk aerosol carbon from Gosan site, Jeju Island in the East China Sea. *Atmos. Environ.* **2014**, *94*, 316−322.
(34) Ceburnis, D.; Garbaras, A.; Szidat, S.; Rinaldi, M.; Fahrni, S.; Perron, N.; Wacker, L.; Leinert, S.; Remeikis, V.; Facchini, M. C.; Prevot, A. S. H.; Jennings, S. G.; O'Dowd, C. D. Quantification of the carbonaceous matter origin in submicron marine aerosol particles by dual carbon isotope analysis. *Atmos. Chem. Phys. Discuss.* **2011**, *11* (1), 2749−2772.
(35) Cachier, H.; Buat-Ménard, P.; Fontugne, M.; Chesselet, R. Long-range transport of continentally-derived particulate carbon in the marine atmosphere: Evidence from stable carbon isotope studies. *Tellus, Ser. B* **1986**, *38B* (3−4), 161−177.
(36) Miyazaki, Y.; Coburn, S.; Ono, K.; Ho, D. T.; Pierce, R. B.; Kawamura, K.; Volkamer, R. Contribution of dissolved organic matter to submicron water-soluble organic aerosols in the marine boundary layer over the eastern equatorial Pacific. *Atmos. Chem. Phys.* **2016**, *16*, 7695−7707.
(37) Chesselet, R.; Fontugne, M.; Buat-Ménard, P.; Ezat, U.; Lambert, C. E. The origin of particulate organic carbon in the marine atmosphere as indicated by its stable carbon isotopic composition. *Geophys. Res. Lett.* **1981**, *8* (4), 345−348.
(38) Miyazaki, Y.; Kawamura, K.; Sawano, M. Size distributions of organic nitrogen and carbon in remote marine aerosols: Evidence of marine biological origin based on their isotopic ratios. *Geophys. Res. Lett.* **2010**, *37* (6), L06803.
(39) Turekian, V. C.; Macko, S. A.; Keene, W. C. Concentrations, isotopic compositions, and sources of size-resolved, particulate organic carbon and oxalate in near-surface marine air at Bermuda during spring. *J. Geophys. Res.* **2003**, *108* (D5), 4157.
(40) Ceburnis, D.; Masalaite, A.; Ovadnevaite, J.; Garbaras, A.; Remeikis, V.; Maenhaut, W.; Claeys, M.; Sciare, J.; Baisnée, D.; O'Dowd, C. D. Stable isotopes measurements reveal dual carbon pools contributing to organic matter enrichment in marine aerosol. *Sci. Rep.* **2016**, *6*, 36675.
(41) Ostrom, N. E.; Macko, S. A.; Deibel, D.; Thompson, R. J. Seasonal variation in the stable carbon and nitrogen isotope biogeochemistry of a coastal cold ocean environment. *Geochim. Cosmochim. Acta* **1997**, *61* (14), 2929−2942.
(42) Savoye, N.; Aminot, A.; Tréguer, P.; Fontugne, M.; Naulet, N.; Kérouel, R. Dynamics of particulate organic matter δ^{15}N and δ^{13}C during spring phytoplankton blooms in a macrotidal ecosystem (Bay of Seine, France). *Mar. Ecol.: Prog. Ser.* **2003**, *255*, 27−41.
(43) Kukert, H.; Riebesell, U. Phytoplankton carbon isotope fractionation during a diatom spring bloom in a Norwegian fjord. *Mar. Ecol.: Prog. Ser.* **1998**, *173*, 127−138.
(44) Stokes, M. D.; Deane, G. B.; Prather, K.; Bertram, T. H.; Ruppel, M. J.; Ryder, O. S.; Brady, J. M.; Zhao, D. A Marine Aerosol Reference Tank system as a breaking wave analogue for the production of foam and sea-spray aerosols. *Atmos. Meas. Tech.* **2013**, *6* (4), 1085−1094.
(45) Guillard, R. R. L.; Ryther, J. H. Studies Of Marine Planktonic Diatoms: I. Cyclotella Nana Hustedt, And Detonula Confervacea (Cleve) Gran. *Can. J. Microbiol.* **1962**, *8* (2), 229−239.
(46) Lee, C.; Sultana, C. M.; Collins, D. B.; Santander, M. V.; Axson, J. L.; Malfatti, F.; Cornwell, G. C.; Grandquist, J. R.; Deane, G. B.; Stokes, M. D.; Azam, F.; Grassian, V. H.; Prather, K. A. Advancing Model Systems for Fundamental Laboratory Studies of Sea Spray Aerosol Using the Microbial Loop. *J. Phys. Chem. A* **2015**, *119* (33), 8860−8870.
(47) Hoefs, J. *Stable Isotope Geochemistry*, 7th ed.; Springer: Cham, Switzerland, 2015; DOI: 10.1007/978-3-319-19716-6.
(48) Lalonde, K.; Middlestead, P.; Gélinas, Y. Automation of $^{13}C/^{12}C$ ratio measurement for fresh water and seawater DOC using high temperature combustion. *Limnol. Oceanogr.: Methods* **2014**, *12* (12), 816−829.
(49) Bligh, E. G.; Dyer, W. J. A Rapid Method of Total Lipid Extraction and Purification. *Can. J. Biochem. Physiol.* **1959**, *37* (8), 911−917.
(50) Quehenberger, O.; Armando, A. M.; Brown, A. H.; Milne, S. B.; Myers, D. S.; Merrill, A. H.; Bandyopadhyay, S.; Jones, K. N.; Kelly, S.; Shaner, R. L.; Sullards, C. M.; Wang, E.; Murphy, R. C.; Barkley, R. M.; Leiker, T. J.; Raetz, C. R.; Guan, Z.; Laird, G. M.; Six, D. A.; Russell, D. W.; McDonald, J. G.; Subramaniam, S.; Fahy, E.; Dennis, E. A. Lipidomics reveals a remarkable diversity of lipids in human plasma. *J. Lipid Res.* **2010**, *51* (11), 3299−3305.
(51) Yuras, G.; Ulloa, O.; Hormazábal, S. On the annual cycle of coastal and open ocean satellite chlorophyll off Chile (18°−40°S). *Geophys. Res. Lett.* **2005**, *32*, No. L23604.
(52) O'Reilly, J. E.; Maritorena, S.; Mitchell, B. G.; Siegel, D. A.; Carder, K. L.; Garver, S. A.; Kahru, M.; Mcclain, C. Ocean color chlorophyll algorithms for SeaWiFS. *J. Geophys. Res.: Oceans* **1998**, *103* (C11), 24937−24953.
(53) O'Dowd, C.; Ceburnis, D.; Ovadnevaite, J.; Bialek, J.; Stengel, D. B.; Zacharias, M.; Nitschke, U.; Connan, S.; Rinaldi, M.; Fuzzi, S.; Decesari, S.; Facchini, M. C.; Marullo, S.; Santoleri, R.; Dell'Anno, A.; Corinaldesi, C.; Tangherlini, M.; Danovaro, R. Connecting marine productivity to sea-spray via nanoscale biological processes: Phytoplankton Dance or Death Disco? *Sci. Rep.* **2015**, *5* (1), 14883.
(54) Rinaldi, M.; Fuzzi, S.; Decesari, S.; Marullo, S.; Santoleri, R.; Provenzale, A.; von Hardenberg, J.; Ceburnis, D.; Vaishya, A.; O'Dowd, C. D.; Facchini, M. C. Is chlorophyll-a the best surrogate for

https://dx.doi.org/10.1021/acsearthspacechem.0c00072
ACS Earth Space Chem. 2020, 4, 1686−1699

organic matter enrichment in submicron primary marine aerosol? *J. Geophys. Res.: Atmos.* **2013**, *118* (10), 4964−4973.
(55) Bird, D. F.; Kalff, J. Empirical Relationships between Bacterial Abundance and Chlorophyll Concentration in Fresh and Marine Waters. *Can. J. Fish. Aquat. Sci.* **1984**, *41* (7), 1015−1023.
(56) Sanders, R.; Caron, D.; Berninger, U. G. Relationships between bacteria and heterotrophic nanoplankton in marine and fresh waters: An inter-ecosystem comparison. *Mar. Ecol.: Prog. Ser.* **1992**, *86*, 1−14.
(57) Kawamura, K.; Ishimura, Y.; Yamazaki, K. Four years' observations of terrestrial lipid class compounds in marine aerosols from the western North Pacific. *Global Biogeochem. Cycles* **2003**, *17* (1), 3-1−3-19.
(58) Beaupre, S. R.; Kieber, D. J.; Keene, W. C.; Long, M. S.; Maben, J. R.; Lu, X.; Zhu, Y.; Frossard, A. A.; Kinsey, J. D.; Duplessis, P.; Chang, R. Y.-W.; Bisgrove, J. Oceanic efflux of ancient marine dissolved organic carbon in primary marine aerosol. *Sci. Adv.* **2019**, *5* (10), eaax6535.
(59) Williams, P. M.; Druffel, E. R. M. Radiocarbon in dissolved organic matter in the central North Pacific Ocean. *Nature* **1987**, *330* (6145), 246−248.
(60) Fry, B.; Hopkinson, C. S.; Nolin, A.; Wainright, S. C. $^{13}C/^{12}C$ composition of marine dissolved organic carbon. *Chem. Geol.* **1998**, *152* (1−2), 113−118.
(61) Miyazaki, Y.; Kawamura, K.; Jung, J.; Furutani, H.; Uematsu, M. Latitudinal distributions of organic nitrogen and organic carbon in marine aerosols over the western North Pacific. *Atmos. Chem. Phys.* **2011**, *11* (7), 3037−3049.
(62) Goericke, R.; Fry, B. Variations of marine plankton $\delta^{13}C$ with latitude, temperature, and dissolved CO2 in the world ocean. *Global Biogeochem. Cycles* **1994**, *8* (1), 85−90.
(63) Hofmann, M.; Wolf-Gladrow, D. A.; Takahashi, T.; Sutherland, S. C.; Six, K. D.; Maier-Reimer, E. Stable carbon isotope distribution of particulate organic matter in the ocean: A model study. *Mar. Chem.* **2000**, *72* (2−4), 131−150.
(64) Hasle, G. R.; Syvertsen, E. E. Marine Diatoms. In *Identifying Marine Phytoplankton*; Tomas, C. R., Ed.; Academic Press: San Diego, CA, 1997; Chapter 2, pp 5−385, DOI: 10.1016/B978-012693018-4/50004-5.
(65) Chingin, K.; Yan, R.; Zhong, D.; Chen, H. Enrichment of Surface-Active Compounds in Bursting Bubble Aerosols. *ACS Omega* **2018**, *3* (8), 8709−8717.
(66) Chingin, K.; Cai, Y.; Liang, J.; Chen, H. Simultaneous Preconcentration and Desalting of Organic Solutes in Aqueous Solutions by Bubble Bursting. *Anal. Chem.* **2016**, *88* (10), 5033−5036.
(67) Modini, R. L.; Russell, L. M.; Deane, G. B.; Stokes, M. D. Effect of soluble surfactant on bubble persistence and bubble-produced aerosol particles. *J. Geophys. Res.: Atmos.* **2013**, *118* (3), 1388−1400.
(68) Walls, P. L. L.; Bird, J. C. Enriching particles on a bubble through drainage: Measuring and modeling the concentration of microbial particles in a bubble film at rupture. *Elem. Sci. Anth.* **2017**, *5*, 34.
(69) Rudolph, J.; Czuba, E.; Huang, L. The stable carbon isotope fractionation for reactions of selected hydrocarbons with OH-radicals and its relevance for atmospheric chemistry. *J. Geophys. Res.: Atmos.* **2000**, *105* (D24), 29329−29346.
(70) Fisseha, R.; Saurer, M.; Jäggi, M.; Siegwolf, R. T.; Dommen, J.; Szidat, S.; Samburova, V.; Baltensperger, U. Determination of primary and secondary sources of organic acids and carbonaceous aerosols using stable carbon isotopes. *Atmos. Environ.* **2009**, *43* (2), 431−437.
(71) Kirillova, E. N.; Andersson, A.; Sheesley, R. J.; Kruså, M.; Praveen, P. S.; Budhavant, K.; Safai, P. D.; Rao, P. S. P.; Gustafsson, Ö. ^{13}C- and ^{14}C-based study of sources and atmospheric processing of water-soluble organic carbon (WSOC) in South Asian aerosols. *J. Geophys. Res.: Atmos.* **2013**, *118* (2), 614−626.
(72) Aggarwal, S. G.; Kawamura, K. Molecular distributions and stable carbon isotopic compositions of dicarboxylic acids and related compounds in aerosols from Sapporo, Japan: Implications for photochemical aging during long-range atmospheric transport. *J. Geophys. Res.* **2008**, *113*, D14301.
(73) Bosch, C.; Andersson, A.; Kirillova, E. N.; Budhavant, K.; Tiwari, S.; Praveen, P. S.; Russell, L. M.; Beres, N. D.; Ramanathan, V.; Gustafsson, Ö. Source-diagnostic dual-isotope composition and optical properties of water-soluble organic carbon and elemental carbon in the South Asian outflow intercepted over the Indian Ocean. *J. Geophys. Res: Atmos.* **2014**, *119* (20), 11,743−11,759.
(74) Dasari, S.; Andersson, A.; Bikkina, S.; Holmstrand, H.; Budhavant, K.; Satheesh, S.; Asmi, E.; Kesti, J.; Backman, J.; Salam, A.; Bisht, D. S.; Tiwari, S.; Hameed, Z.; Gustafsson, Ö Photochemical degradation affects the light absorption of water-soluble brown carbon in the South Asian outflow. *Sci. Adv.* **2019**, *5* (1), eaau8066.
(75) Tritscher, T.; Dommen, J.; Decarlo, P. F.; Gysel, M.; Barmet, P. B.; Praplan, A. P.; Weingartner, E.; Prévôt, A. S. H.; Riipinen, I.; Donahue, N. M.; Baltensperger, U. Volatility and hygroscopicity of aging secondary organic aerosol in a smog chamber. *Atmos. Chem. Phys.* **2011**, *11* (22), 11477−11496.
(76) Farmer, D. K.; Cappa, C. D.; Kreidenweis, S. M. Atmospheric Processes and Their Controlling Influence on Cloud Condensation Nuclei Activity. *Chem. Rev.* **2015**, *115* (10), 4199−4217.

https://dx.doi.org/10.1021/acsearthspacechem.0c00072
ACS Earth Space Chem. 2020, 4, 1686−1699